

Journal of Visualized Experiments

Real-time imaging of CCL5-induced migration of periosteal skeletal stem cells in a living animal

--Manuscript Draft--

Article Type:	Methods Article - JoVE Produced Video
Manuscript Number:	JoVE61162R1
Full Title:	Real-time imaging of CCL5-induced migration of periosteal skeletal stem cells in a living animal
Section/Category:	JoVE Biology
Keywords:	Periosteum; Intravital Microscopy; cell migration; skeletal stem cell; fracture healing
Corresponding Author:	Dongsu Park, Ph.D. Baylor College of Medicine Houston, TX UNITED STATES
Corresponding Author's Institution:	Baylor College of Medicine
Corresponding Author E-Mail:	Dongsu.Park@bcm.edu
Order of Authors:	Laura Ortinu Kevin Lei Youngjae Jeong Dongsu Park
Additional Information:	
Question	Response
Please indicate whether this article will be Standard Access or Open Access.	Standard Access (US\$2,400)
Please indicate the city, state/province, and country where this article will be filmed. Please do not use abbreviations.	Houston, Texas, United States of America

TITLE:

Real-Time Imaging of CCL5-Induced Migration of Periosteal Skeletal Stem Cells in Mice

AUTHORS AND AFFILIATIONS:

Laura Ortinau^{1,2}, Kevin Lei¹, Youngjae Jeong¹, Dongsu Park^{1,2,3}

¹Department of Molecular & Human Genetics, Baylor College of Medicine, Houston, TX, USA

²Center for Skeletal Biology, Baylor College of Medicine, Houston, TX, USA

³Department of Pathology & Immunology, Baylor College of Medicine, Houston, TX, USA

Corresponding Author:

Dongsu Park (dongsu.park@bcm.edu)

Email Addresses of Co-authors:

Laura Ortinau (laura.ortinau@bcm.edu)

Kevin Lei (kevin.lei@bcm.edu)

Youngjae Jeong (youngjae.jeong@bcm.edu)

KEYWORDS:

periosteum, skeletal stem cells, migration, intravital imaging, P-SSC, CCR5

SUMMARY:

This protocol describes the detection of CCL5-mediated periosteal skeletal stem cell migration in real-time using live animal intravital microscopy.

ABSTRACT:

Periosteal skeletal stem cells (P-SSCs) are essential for lifelong bone maintenance and repair, making them an ideal focus for the development of therapies to enhance fracture healing. Periosteal cells rapidly migrate to an injury to supply new chondrocytes and osteoblasts for fracture healing. Traditionally, the efficacy of a cytokine to induce cell migration has only been conducted in vitro by performing a transwell or scratch assay. With advancements in intravital microscopy using multiphoton excitation, it was recently discovered that 1) P-SSCs express the migratory gene CCR5 and 2) treatment with the CCR5 ligand known as CCL5 improves fracture healing and the migration of P-SSCs in response to CCL5. These results have been captured in real-time. Described here is a protocol to visualize P-SSC migration from the calvarial suture skeletal stem cell (SSC) niche towards an injury after treatment with CCL5. The protocol details the construction of a mouse restraint and imaging mount, surgical preparation of the mouse calvaria, induction of a calvaria defect, and acquisition of time-lapse imaging.

INTRODUCTION:

Fracture repair is a dynamic, multicellular process that is distinct from embryonic skeletal development and remodeling. During this process, the induction of injury signals from damaged tissue is followed by the rapid recruitment, proliferation, and subsequent differentiation of

skeletal stem/progenitor cells, which are all critical for the overall stability and fixation of fractures¹. In particular, early stages of fracture healing require soft callus formation, which is mainly attributed to periosteal resident cells². When bones are injured, a subset of periosteal cells rapidly respond and contribute to newly differentiated cartilage intermediates and osteoblasts within the callus³, implicating the presence of a distinct skeletal stem/progenitor cell population within the periosteum. Therefore, the identification and functional characterization of the periosteum-resident skeletal stem cells (SSCs) constitute a promising therapeutic approach for degenerative bone diseases and bone defects⁴.

SSCs are thought to reside in multiple tissue locations, including the bone marrow. Similar to bone marrow, osteogenic/chondrogenic SSCs have also been identified in the periosteum⁴⁻⁶. These periosteal SSCs (P-SSCs) can be labeled with early mesenchymal lineage markers (i.e., *Prx1*-Cre⁵, *Ctsk*-Cre⁷, and *Axin2*-CreER⁸) during fetal bone development^{4,7-10}. A significant limitation of these single genetic lineage tracing models is that there is substantial heterogeneity within labeled cell populations. Furthermore, they cannot distinguish labeled SSCs from their progeny in vivo. To address this limitation, we recently developed a dual reporter mouse (*Mx1*-Cre⁺*Rosa26*-Tomato⁺ α SMA-GFP⁺) to distinctly visualize P-SSCs from bone marrow SSCs (BM-SSCs)¹¹. With this model, it has been determined that P-SSCs are marked by *Mx1*⁺ α SMA⁺ dual labeling, whereas more differentiated *Mx1*⁺ cells reside in the bone marrow, endosteal and periosteal surfaces, and cortical and trabecular bones^{11,12}.

Multiple cytokines and growth factors are known to regulate bone remodeling and repair and have been tested for the enhancement of skeletal repair in critical segment defects^{1,13}. However, due to the cellular complexity of injury models generated through disruption of the bone compartment's physical barrier, the direct effects of these molecules on endogenous P-SSC migration and activation during healing are unclear. The functional characteristics and migratory dynamics of SSCs are often assessed in vitro by performing a transwell or scratch assay, in combination with cytokines or growth factors known to induce migration in other cell populations. Thus, interpretation of results from these in vitro experiments for application in their corresponding in vivo systems is challenging. Currently, in vivo assessment of skeletal stem/progenitor cell migration is not typically observed in real-time; rather, it is measured at fixed timepoints post-fracture^{5,7,14-16}.

A limitation of this method is that migration is not assessed at a single-cell level; rather, it is measured via changes in cell populations. Due to recent advances in live animal intravital microscopy and generation of additional reporter mice, in vivo tracking of individual cells is now possible. Using live animal intravital microscopy, we observed the distinct migration of P-SSCs from the calvaria suture niche to a bone injury within 24–48 h post-injury in *Mx1*/Tomato/ α SMA-GFP mice.

CCL5/CCR5 was recently identified as a regulatory mechanism influencing the recruitment and activation P-SSCs during the early injury response. Interestingly, there was no detection of substantial P-SSC migration in response to an injury in real-time. However, treatment of an injury with CCL5 produces a robust, directionally distinct migration of P-SSCs, which can be

captured in real-time. Therefore, the objective of this protocol is to provide a detailed methodology for recording the in vivo migration of P-SSCs in real-time after treatment with CCL5.

PROTOCOL:

All mice were maintained in pathogen-free conditions, and all procedures were approved by Baylor College of Medicine's Institutional Animal Care and Use Committee (IACUC).

1. Mouse preparation

1.1. Cross *Mx1-Cre*¹⁷ and *Rosa26-loxP-stop-loxP-tdTomato* (Tom)¹⁸ mice (purchased from the Jackson Laboratory) with α SMA-GFP mice (provided here by Drs. Ivo Kalajzic and Henry Kronenberg) to generate *Mx1-Cre*⁺*Rosa26-Tomato*⁺ α SMA-GFP⁺ (Mx1/Tomato/ α SMA-GFP) reporter mice (**Figure 2A**).

1.2. For *Mx1-Cre* induction, inject mice with 25 mg/kg plpC every other day for 10 days.

1.3. Irradiate mice with 9.5 Gy 1 day prior to intravenous transplantation of 1×10^6 whole bone marrow mononuclear cells from wild-type C57BL/6 mice (WT-BMT)¹⁹.

1.4. After 6 to 8 weeks of recovery, subject mice to the in vivo imaging of periosteal cell migration protocol described below.

NOTE: Irradiation and WT-BMT of *Mx1-Cre* mice are necessary to eliminate endogenously *Mx1*-labeled hematopoietic cells that may respond to an injury. Six to eight weeks post-irradiation, the host's hematopoietic cell count is at >5% and thus ready for imaging¹⁹.

2. Mouse restraint and imaging mount

2.1. Create a mouse restraint with a 50 mL conical tube (**Figure 1A**).

2.1.1. Using pointed scissors, poke a hole through the bottom of the conical. Cut from the bottom hole to the top of the conical (the cut side will be the top of the restraint).

2.1.2. Make a cut approximately 4–5 cm long parallel to the previous cut and halfway down (~2 cm) from the top of the restraint. Remove this section of the conical and smooth the edges were necessary.

2.2. Construct a conical tube imaging mount using an adjustable angle plate, a 0.5" optical post, and a right-angle clamp for the 0.5" post, 0.1875" Hex (**Figure 1B** and **Table of Materials**).

2.2.1. Adjust the angle plate to a 35° angle. On the left side of the angle plate, screw the optical post into the second hole from the back of the plate.

2.2.2. On the right side of the adjustable plate, insert a spring-loaded 0.1875" Hex-locking 0.25" thumbscrew into the second hole from the front and last holes on the plate. The right-angle clamp will be used with the optical post to secure the conical mouse restraint in place.

3. Preoperative surgical procedure

3.1. Mouse anesthesia

3.1.1. For pain management, subcutaneously inject the mouse with sustained release buprenorphine (1 mg/kg BW) 30–60 min prior to surgery.

3.1.2. Anesthetize mice using rodent III CCM combination (combo III) anesthesia containing 37.5 mg/mL ketamine, 1.9 mL/mg xylazine, and 0.37 mg/mL acepromazine. The appropriate dosage for mice is 0.75–1.50 mL per 1 kg of body weight. The dose will last 30–45 min.

3.1.3. Once the mouse is anesthetized, apply ophthalmic ointment to the eyes with a sterile cotton swab to prevent eye dehydration.

3.1.4. For long-term imaging (>45 min), administer anesthesia again to maintain proper anesthetic depth as follows.

3.1.4.1. Prepare a 1 mL syringe with a sufficient amount of combo III to maintain anesthesia for the planned imaging duration (0.75 mL/kg BW per 30 min of additional sedation). Attach a 25 G butterfly needle infusion set with 12" tubing to the syringe and push anesthetic through the tubing and needle.

3.1.4.2. Insert the butterfly needle intraperitoneally, then tape the needle in place.

NOTE: This is how the additional combo III will be administered during imaging such that there is no need to move the animal or disrupt the plane of view.

3.2. Mouse restraint and preparation of the surgical site

3.2.1. Use clippers to remove as much hair as possible from the top of the head. Apply depilatory cream to the shaved area to remove any remaining hair at the surgical site.

3.2.2. Ensure that the mouse is fully anesthetized by a lack of response to toe pinches. After 15 min, if the mouse is not fully anesthetized, administer a second smaller dose of combo III (<0.75 mL/kg BW).

3.2.3. Place the mouse in the restraint tail-first, sliding it far enough backwards such that the nose slightly hangs over the edge of the conical.

3.2.4. Tape the front paws to the bottom of the conical tube using medical tape.

3.2.5. Place conical tube with mouse on an imaging mount that is set at a 35° angle and secure using the right-angle clamp (**Figure 1C**).

3.2.6. Once the mouse is secure in the imaging mount, clean the surgical site 3x with alternating scrubs of betadine scrub and 70% isopropyl alcohol. Again, check that the animal is fully sedated.

3.2.7. Move the mouse to a clean absorbent pad and place a drape over the mouse to create a large sterile field.

4. Surgical procedure

4.1. Opening incision

4.1.1. Using fine-tipped forceps, pick up the skin immediately medial to the right ear. With microdissection scissors, cut the skin being held by the forceps.

NOTE: Initiating the incision using the method described above creates a rounded incision that is more suitable for suturing after the procedure.

4.1.2. Make a transverse incision starting from the initial incision toward the left ear (<1 cm). Make another incision, starting from the initial incision, towards the nose of the animal (~2–3 mm past the right eye).

4.1.3. Separate the skin from the periosteum using the forceps and scissors to gently cut through the connective tissue separating the skin from calvaria periosteum.

4.1.4. Using a sterile cotton swab, apply some ophthalmic ointment to the top of the skin flap. Gently pick up the skin flap and fold it over the left eye. The intersection of the sagittal and coronal sutures should be clearly exposed (**Figure 1E**).

NOTE: The ophthalmic ointment is used to keep the skin flap in place.

4.1.5. Flush the open surface with sterile PBS to clean the area of any blood and residual hair.

NOTE: If necessary, use fine-tipped forceps to remove hairs that remain after flushing, but be careful not to damage the periosteum.

4.2. Microfracture

4.2.1. To generate microfractures on the calvaria, remove the plunger of a 29 G insulin syringe and cut the back end of the syringe, around the 300–400 uL marks.

NOTE: This step makes it easier to maneuver under a dissection scope when producing the injury.

4.2.2. Place the tip of a bevel (one to two needle widths) towards the nose from the coronal suture and one to two needle widths to the right of the sagittal suture (**Figure 1E**).

4.2.3. Gently rotate the syringe clockwise, then counterclockwise several times.

NOTE: In young mice, a very small amount of downward pressure is needed to create a circular microfracture. Be careful not to let the needle penetrate the brain, as this will cause bleeding and interfere with imaging.

4.2.4. Use a 27 G needle to widen the microfracture to ~0.4 mm. If bone fragments remain in the microfracture, flush the area with PBS. If bone fragments still remain in the microfracture, use the 29 G needle to gently scoop them out.

4.2.5. Repeat steps 4.2.1–4.2.4 to create an injury on the left side of the sagittal suture.

NOTE: At this point, there are two options: 1) immediately proceed to CCL5 treatment (section 4.3) and imaging (section 5); or 2) close the surgical site following the postoperative procedures in section 6. At 24 h later, anesthetize the mouse again, reopen the surgical sight, treat the injury with CCL5 (section 4.3), and perform intravital imaging (section 5) and postoperative care (section 6).

4.3. CCL5 treatment

4.3.1. From a stock of RANTES (100 ng/mL), make a solution of 10 ng/mL using basement membrane matrix (**Table of Materials**). Keep this solution on ice to keep the matrix in liquid form.

4.3.2. Treat each injury with 2 μ L of CCL5 (10 ng/ μ L) by using a 2-20 μ L pipette (this pipette tip has a larger diameter, which is more effective when using a viscous liquid). Allow the matrix to solidify.

4.3.3. Once the matrix has solidified, gently cover the calvaria with the skin flap to ensure the tissue does not become dehydrated. Incubate for 1 h prior to imaging.

5. Intravital imaging

5.1. Microscope settings

5.1.1. Turn on the multiphoton laser (femtosecond titanium-sapphire laser). Set the wavelength to 880 nm and adjust the power for second harmonic generation (SHG) imaging (440 nm) of the

bone.

5.1.2. Turn on the 488 nm and 561 nm solid state lasers for excitation of GFP- and tdTomato-expressing cells, respectively.

5.1.3. Turn on PMT (photomultiplier tube) detectors for second harmonic generation (405–455 nm detection) and GFP (505–550 nm detection) signals. Turn on HyD 3 detector for tomato (590–620 nm detection) signal.

5.2. Mounting

5.2.1. Before moving the mouse to the scope, check the visual plane of the calvaria by gently pressing the back of the mouse's head. If the plane is not level, adjust the position by gently rotating the mouse restraint to the left or the right.

NOTE: This is a critical step to ensure sufficient image quality.

5.2.2. Apply sterile 2% methylcellulose in water (w/v) to cover the entire calvaria and skin flap and prevent drying of the tissue.

5.2.3. Place the mouse on the XYZ-axis motorized microscope stage (**Figure 1G**). Using the epifluorescent light, align the mouse so that 1) it is facing the microscope and 2) the intersection of the coronal and sagittal sutures are the centered reference point of the stage.

5.2.4. Place the glass cover on the imaging area and double-check the alignment (**Figure 1H**).

5.3. Time-lapse imaging

5.3.1. Use a low magnification lens (25x water immersion objective with NA = 0.95) to scan the calvaria. Acquire a reference image of the sagittal and coronal suture intersection.

5.3.2. Using the SHG and fluorescent signals from the cells, locate each injury sight and record the XYZ coordinates as well as the distances from the sagittal and coronal sutures (**Figure 2B**).

5.3.3. Pick a location on either the coronal or sagittal sutures for long-term imaging. Take a detailed Z-stack image of this area from reference during imaging.

NOTE: Since the sutures represent a known P-SSC niche, this is where the cells will be migrating from in response to the calvaria injury.

5.3.4. Use the time-lapse software settings to record an image every 1 min for at least 1 h. In the time between snapshots, compare the current field of view with the initial field of view. If they are different, use the Z-stack image to determine in which direction the field of view needs to be adjusted.

6. Postoperative animal care

6.1. After imaging, rinse the exposed calvaria with sterile PBS to remove the methylcellulose.

6.2. To close the incision, gently place the skin flap over the calvaria. Use sterile cotton swabs to remove residual ophthalmic ointment and dry the incision site.

6.3. Using monofilament nylon 5-0 size nonabsorbable sutures with an attached C-1 reverse cutting needle, close the surgical site. Use a sterile cotton swab to apply triple antibiotic ointment to the closed incision.

NOTE: Scarring is reduced with high quality suturing techniques.

6.4. Place mouse in a clean cage on a warm surface and check every 15 min until sternal recumbency is achieved.

6.5. Administer a second dose of sustained release buprenorphine 72 h post-surgery.

6.6. Monitor daily for huddling behavior, ruffled fur, and/or lack of ambulation until sutures are removed (~1 week).

REPRESENTATIVE RESULTS:

Skeletal progenitors have been proposed to have migratory or circulatory potential²⁰. Recently, *Mx1-Cre⁺Rosa26-Tomato⁺ α SMA-GFP⁺* (*Mx1/Tomato/ α SMA-GFP*) reporter mice were generated, in which P-SSCs are marked by *Mx1⁺ α SMA⁺* dual labeling (**Figure 2A,B**). Substantial migration of *Mx1⁺ α SMA⁺* P-SSCs occurred out of the suture mesenchyme within 24–48 h post-injury¹¹. Also tested was the possibility of detecting in vivo P-SSC migration in real-time 24 h after a calvaria defect. Little to no migration of *Mx1⁺ α SMA⁺* P-SSCs was observed within 1 h of imaging (**Figure 2C**).

Mx1⁺ α SMA⁺ P-SSCs uniquely express the CCL5 receptor known as CCR5¹¹. Thus, treatment of a calvaria defect 24 h post-injury with CCL5 induced directionally distinct migration away from the coronal suture and towards the injury sight (**Figure 2D,E**). Within 1 h of imaging, one of the *Mx1⁺ α SMA⁺* P-SSCs migrated approximately 50 μ m toward the injury (**Figure 2E**). Other *Mx1⁺ α SMA⁺* P-SSCs were also observed migrating in response to CCL5 treatment but to a lesser extent.

FIGURE AND TABLE LEGENDS:

Figure 1: Set-up for in vivo imaging of mouse calvaria. Representative images of the mouse restraint (**A**) and imaging mount (**B**) used during live imaging. (**C**) Mouse in the restraint and secured to the imaging mount. (**D**) Schematic representation of mouse calvaria structure,

identifying the frontal (FS), coronal (CS), sagittal (SS), and lambdoid (LS) sutures. (E) Representative placement of calvaria microfracture injuries. (F) Postoperative surgical suture placement for optimal healing and future imaging. Representative images of mount placement on microscope stage (G) and coverslip placement (H).

Figure 2: Real-time in vivo imaging of $Mx1^{+}\alpha SMA^{+}$ P-SSC migration. (A) Schematic of $Mx1$ /Tomato/ αSMA -GFP dual reporter mice preparation. Mice were injected intraperitoneally with 25 mg/kg plpC every other day for 10 days (1). $Mx1$ /Tomato/ αSMA -GFP mice were lethally irradiated with 9.5 Gy (2) 1 day before intravenous transplantation of 1×10^6 whole bone marrow mononuclear cells from WT C57BL/6 mice (3). After 6–8 weeks of recovery (when the host's hematopoietic cells were less than 5%), mice were subjected to bone injury experiments. $Mx1^{+}$ (Tomato⁺), αSMA^{+} (GFP⁺), $Mx1^{+}\alpha SMA^{+}$ (Tomato⁺GFP⁺), and bone (blue). (B) Maximum Z-projection of a representative calvaria injury (white circle) and imaging (white square) locations in relation to sagittal (SS) and coronal (CS) sutures of $Mx1$ /Tomato/ αSMA -GFP mouse. Dotted lines represent calvaria sutures. (C) In vivo imaging of $Mx1^{+}\alpha SMA^{+}$ P-SSCs response 24 hours post-injury. Scale bar = 25 μm . (D) 24 h post-injury, CCL5 was administered at the injury sight, and in vivo imaging was performed 1 h later in relation to the coronal suture (CS). White square represents location of cell migration images shown in (E). Scale bar = 75 μm . (E) Migration of $Mx1^{+}\alpha SMA^{+}$ P-SSCs on the bone (blue) surface toward the injury sight (top right). Scale bar = 25 μm . In (C,D,E), the numbers indicate the time of imaging. Yellow arrow indicates the direction of injury location. Asterisk indicates the migratory path of $Mx1^{+}\alpha SMA^{+}$ P-SSC. The image is representative of results from three to five mice.

DISCUSSION:

During bone healing, periosteal cells are the main source of newly differentiated chondrocytes and osteoblasts within an injury callus³. Similar to bone marrow, osteogenic/chondrogenic SSCs have also been identified in the periosteum^{4–6}. Assessing endogenous P-SSC functional characteristics is technically challenging. Often, migratory dynamics of SSCs are assessed in vitro, making interpretation of their corresponding in vivo systems challenging. Due to recent advances in live animal intravital microscopy and generation of additional reporter mice ($Mx1$ /Tomato/ αSMA -GFP), in vivo tracking of individual cells is now possible. Thus, this method allows the in vivo recording of CCL5 induced P-SSCs migration in real-time.

There are several technical challenges associated with this method that can influence imaging consistency. A major technical challenge with this method is maintaining the Z-axis plane of view. Z-axis drift (Z-drift) is a common issue in long-term imaging of fixed and live samples, and it is largely attributed to temperature changes in the imaging environment. Although this artifact cannot be completely counteracted, covering the stage, objective lenses, and supporting structures helps to reduce Z-drift²¹.

Furthermore, obtaining a Z-stack series of the imaging location prior to time-lapse imaging will establish a reference of the Z-axis that can be referred to between image acquisitions (i.e., images are typically taken every 30-60 s, which allows time for adjustments to the Z-axis, if

necessary). Another technical challenge is making a consistent microfracture that is the same size, shape, and distance from the calvaria sutures. The distance from the coronal and sagittal sutures is critical, because the calvaria sutures are a niche for quiescent SSCs¹⁰. The best method to reduce variability of the microfracture is to practice this technique in mice that are not included in the final analysis.

Despite the limitations, this method provides a unique system to assess individual cellular response in vivo to a bone injury. Since fracture repair is a highly complex processes involving multiple cell types, there are several aspects that are not fully understood. One of these includes the early migratory response of P-SSCs toward an injury. While CCR5/CCL5 is a unique mechanism by which P-SSCs are recruited to an injury, it is possible that additional cytokines and growth factors play an important role in fracture healing. Previously, the treatment of fractures with various cytokines and growth factors has resulted in highly variable outcomes in overall fracture healing²². This imaging method provides a unique platform to determine the physiological effects of potential drug/cytokine/growth factor therapies on individual cellular responses. Finally, it provides in vivo mechanistic data that can support a specific therapy's enhancement of fracture healing.

ACKNOWLEDGMENTS:

This work was supported by the Bone Disease Program of Texas Award, the Caroline Wiess Law Fund Award, and the NIAMS of the National Institutes of Health under award numbers 1K02AR061434 and 1R01AR072018 to D.P. We thank M.E. Dickinson and T.J. Vadakkan in the BCM Optical Imaging and Vital Microscopy Core.

DISCLOSURES:

L.C.O. and D.P. disclose a pending patent entitled "Periosteal Skeletal Stem Cells in Bone Repair" (BAYM.P0264US.P1). The remaining authors declare no competing interests.

REFERENCES:

1. Einhorn, T. A., Gerstenfeld, L. C. Fracture healing: mechanisms and interventions. *Nature Reviews Rheumatology*. **11** (1), 45–54 (2015).
2. Murao, H., Yamamoto, K., Matsuda, S., Akiyama, H. Periosteal cells are a major source of soft callus in bone fracture. *Journal of Bone and Mineral Metabolism*. **31** (4), 390–398 (2013).
3. Colnot, C. Skeletal cell fate decisions within periosteum and bone marrow during bone regeneration. *Journal of Bone and Mineral Research*. **24** (2), 274–282 (2009).
4. Roberts, S. J., van Gestel, N., Carmeliet, G., Luyten, F. P. Uncovering the periosteum for skeletal regeneration: the stem cell that lies beneath. *Bone*. **70**, 10–18 (2015).
5. Duchamp de Lageneste, O. *et al.* Periosteum contains skeletal stem cells with high bone regenerative potential controlled by Periostin. *Nature Communications*. **9** (1), 773 (2018).
6. Olivos-Meza, A. *et al.* Pretreatment of periosteum with TGF-beta1 in situ enhances the quality of osteochondral tissue regenerated from transplanted periosteal grafts in adult rabbits. *Osteoarthritis Cartilage*. **18** (9), 1183–1191 (2010).
7. Debnath, S. *et al.* Discovery of a periosteal stem cell mediating intramembranous bone

formation. *Nature*. **562** (7725), 133–139 (2018).

8. Ransom, R. C. *et al.* Axin2-expressing cells execute regeneration after skeletal injury. *Scientific Reports*. **6**, 36524 (2016).
9. Ouyang, Z. *et al.* Prx1 and 3.2kb Col1a1 promoters target distinct bone cell populations in transgenic mice. *Bone*. **58**, 136–145 (2013).
10. Wilk, K. *et al.* Postnatal Calvarial Skeletal Stem Cells Expressing PRX1 Reside Exclusively in the Calvarial Sutures and Are Required for Bone Regeneration. *Stem Cell Reports*. **8** (4), 933–946 (2017).
11. Ortinau, L. C. *et al.* Identification of Functionally Distinct Mx1+alphaSMA+ Periosteal Skeletal Stem Cells. *Cell Stem Cell*. **25** (6), 784–796.e5 (2019).
12. Devez, L., Ortinau, L., Lei, K., Park, D. Comparative analysis of gene expression identifies distinct molecular signatures of bone marrow- and periosteal-skeletal stem/progenitor cells. *PLoS One*. **13** (1), e0190909 (2018).
13. Schindeler, A., McDonald, M. M., Bokko, P., Little, D. G. Bone remodeling during fracture repair: The cellular picture. *Seminars in Cell and Developmental Biology*. **19** (5), 459–466 (2008).
14. Shi, Y. *et al.* Gli1 identifies osteogenic progenitors for bone formation and fracture repair. *Cell Stem Cell*. **15** (2), 782–796 (2017).
15. Zhou, B. O., Yue, R., Murphy, M. M., Peyer, J. G., Morrison, S. J. Leptin-receptor-expressing mesenchymal stromal cells represent the main source of bone formed by adult bone marrow. *Cell Stem Cell*. **15** (2), 154–168 (2014).
16. Grcevic, D. *et al.* In vivo fate mapping identifies mesenchymal progenitor cells. *Stem Cells*. **30** (2), 187–196 (2012).
17. Kuhn, R., Schwenk, F., Aguet, M., Rajewsky, K. Inducible gene targeting in mice. *Science*. **269** (5229), 1427–1429 (1995).
18. Srinivas, S. *et al.* Cre reporter strains produced by targeted insertion of EYFP and ECFP into the ROSA26 locus. *BMC Developmental Biology*. **1**, 4 (2001).
19. Park, D. *et al.* Endogenous bone marrow MSCs are dynamic, fate-restricted participants in bone maintenance and regeneration. *Cell Stem Cell*. **10** (3), 259–272 (2012).
20. Nitzsche, F. *et al.* Concise Review: MSC Adhesion Cascade-Insights into Homing and Transendothelial Migration. *Stem Cells*. **35** (6), 1446–1460 (2017).
21. Adler, J., Pagakis, S. N. Reducing image distortions due to temperature-related microscope stage drift. *Journal of Microscopy*. **210** (Pt 2), 131–137 (2003).
22. Roberts, S. J., Ke, H. Z. Anabolic Strategies to Augment Bone Fracture Healing. *Current Osteoporosis Reports*. **16** (3), 289–298 (2018).

Figure 1

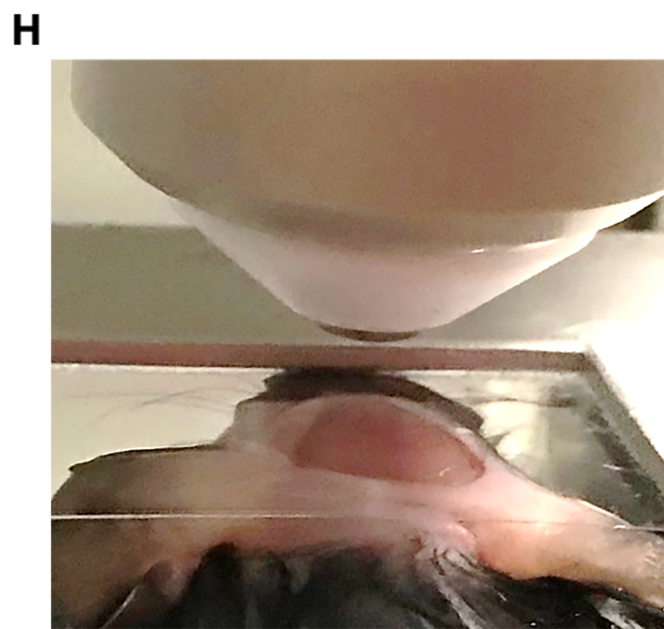
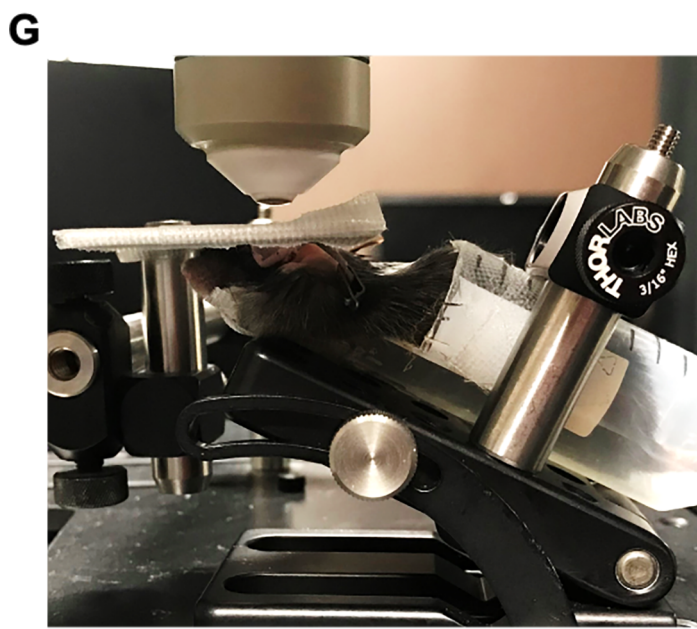
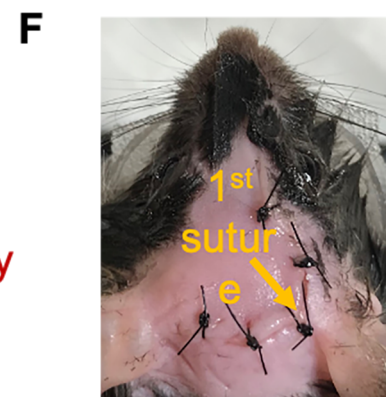
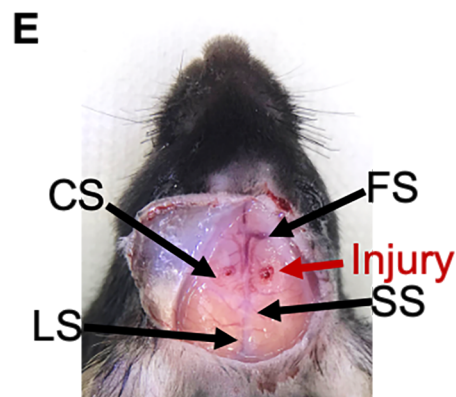
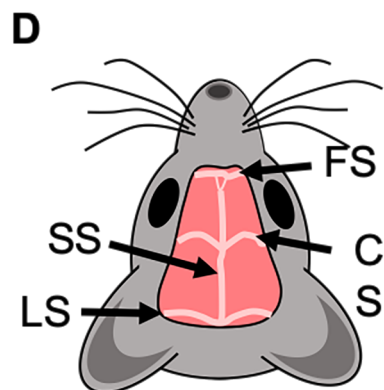
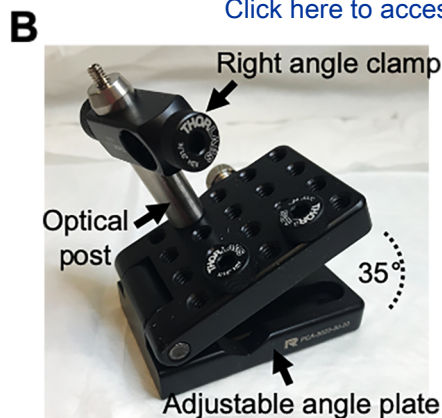
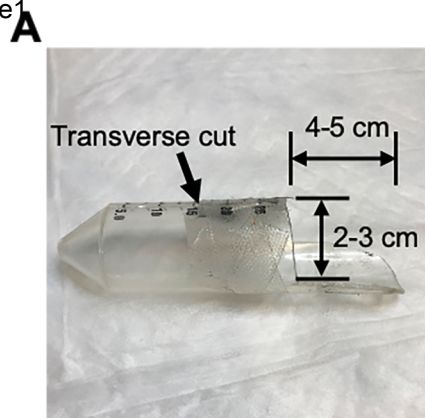
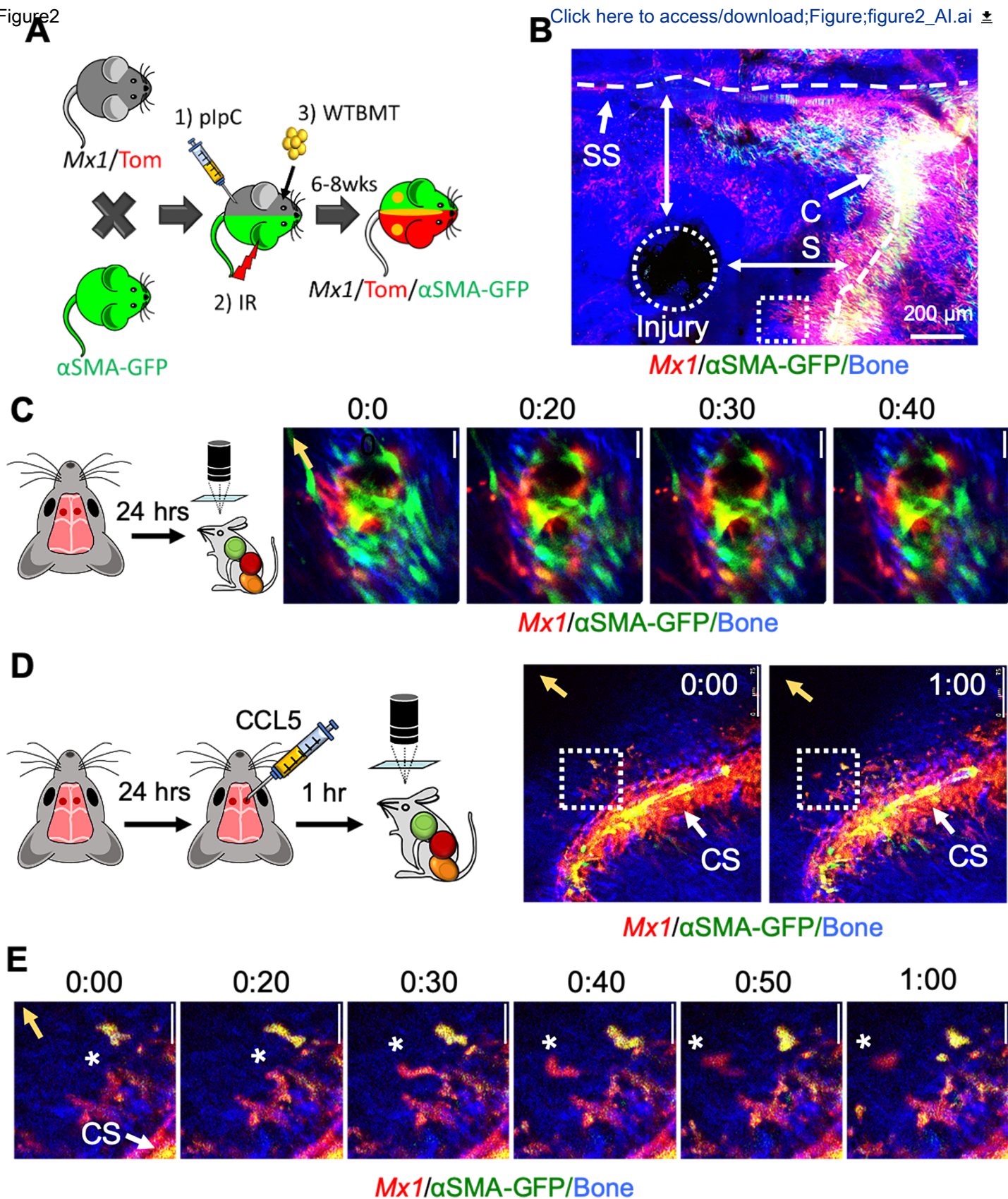
[Click here to access/download;Figure;figure1_AI.ai](#)

Figure 2

[Click here to access/download;Figure;figure2_Al.ai](#)


Name of Material/ Equipment	Company	Catalog Number	Comments/Description
½" optical post	ThorLabs	TR2	For imaging mount
1 mL syringe	BD	309659	
27G needle	BD PercisionGlide	305111	
29G insulin syringe	McKesson	102-SN05C905P	
50 mL conical tube	Falcon	352098	For mouse restraint
Adjustable angle plate	Renishaw	R-PCA-5023-50-20	For imaging mount
Alcohol wipes	Coviden	6818	
betadine surgical scrub	Henry Schen	67618-151-16	
Buprenorphine SR-LAB	ZooPharm		1mg/mL Sustained Release
Combo III	Obtained from staff veterinarian	N/A	37.6 mg/mL Ketamine; 1.9 mg/mL Xylazine; 0.37 mg/mL Acepromazine
Coverslip	Fisher	12-545-87	24 x 40 premium superslip
Fine tip forceps	FST	11254-20	
Ketamine	KetaVed	50989-161-06	100 mg/mL
Leica TCS SP8MP with DM6000CFS	Leica Microsystems	N/A	
Matrigel	R & D Systems	344500101	
Medical tape	McKesson	100199	3" x 10 yds (7.6 cm x 9.1 m)
Methocellulose	Electron Microscopy Sciences	19560	
Microdissection scissors	FST	1456-12	
Motorized stage	Anaheim automation	N/A	
Needle holder	FST	12500-12	
Nonabsorbable sutures	McKesson	S913BX	monofilament nylon 5-0 nonabsorbable sutures with attached C-1 reverse cutting needle
Ophthalmic ointment	Rugby	0536-1086-91	
RANTES	Biolegend	594202	10 µg/50 µL
Right-angle clamp for ½" post, 3/16" Hex	ThorLabs	RA90	For imaging mount
Spring-loaded 3/16" Hex-locking ¼" thumbscrew	ThorLabs	TS25H	For imaging mount
Sterile cotton swabs	Henry Schen	100-9249	
Sterile DPBS (1x)	Corning	21-030-CV	
Sterile drapes	McKesson	25-517	
Surgical gloves	McKesson	3158VA	
Triple antibiotic ointment	Taro Pharmaceuticals U.s.a., Inc.	51672-2120-2	
Vacutainer blood collection set	BD	REF 367298	25G butterfly needle infusion set with 12" tubing

February 20, 2020

RE: JoVE61162

Dear Dr. Phillip Steindel,

Thank you for the opportunity to respond to the remaining concerns of the reviewers. We have made substantial modifications to the manuscript, with addition of new data, and detail below (in blue) our response to the comments made by the editor and the reviewers:

Editorial comments:

General:

1. Please take this opportunity to thoroughly proofread the manuscript to ensure that there are no spelling or grammar issues.
2. Please ensure that the manuscript is formatted according to JoVE guidelines—letter (8.5" x 11") page size, 1-inch margins, 12 pt Calibri font throughout, all text aligned to the left margin, single spacing within paragraphs, and spaces between all paragraphs and protocol steps/substeps.
3. Please provide at least 6 key words or phrases.
4. JoVE cannot publish manuscripts containing commercial language. This includes trademark symbols (™), registered symbols (®), and company names before an instrument or reagent. Please limit the use of commercial language from your manuscript and use generic terms instead. All commercial products should be sufficiently referenced in the Table of Materials and Reagents.

For example: Matrigel

Protocol:

1. Please split up longer Protocol steps into smaller steps/substeps; individual steps should contain only 2–3 actions and a maximum of 4 sentences.
2. For each protocol step/substep, please ensure you answer the “how” question, i.e., how is the step performed? Alternatively, add references to published material specifying how to perform the protocol action. If revisions cause a step to have more than 2-3 actions and 4 sentences per step, please split into separate steps or substeps.

Specific Protocol steps:

1. 1.a: How are mice irradiated?

Figures:

1. If necessary, please obtain explicit copyright permission to reuse any figures from a previous publication. Explicit permission can be expressed in the form of a letter from the editor or a link to the editorial policy that allows re-prints. Please upload this information as a .doc or .docx file to your Editorial Manager account. The Figure must be cited appropriately in the Figure Legend, i.e. “This figure has been modified from [citation].”

References:

1. Please do not abbreviate journal titles.

Table of Materials:

1. Please ensure the Table of Materials has information on all materials and equipment used, especially those mentioned in the Protocol.

Reviewers' comments:

Reviewer #1:

Manuscript Summary:

For in vivo tracking of individual skeletal stem/progenitor cells, this is a very well conducted, impressive technique. The manuscript contains lots of robust, clear and convincing protocols. Manuscript is well written and I only have a few comments to improve this submission.

Minor Concerns:

In my understanding, Fig. 2D showed images one hour before and after CCL5 administration at the injury site and the first and last photos in Fig. 2E showed matched photos for 0:00 and 1:00 dashed box of Fig. 2D. However, both images in Fig. 2D look quite similar. The authors need to make sure that these images pointed before and after CCL5 administration.

We appreciated the reviewers comment and have replace the 1:00 after CCL5 administration image in figure 2D with the appropriate corresponding image in 2E.

Reviewer #2:

Manuscript Summary:

This is a nice piece of story to highlight a cutting edge technique for intravital bone imaging. Needless to say, live imaging is by far informative than snap shots, but doing so in bone is quite hustle by several reasons. The authors are pioneers of this imaging technique and they describe this technique step-by-step in this manuscript. They also show a new piece of information that skeletal stem cells migrate towards an injury site in vivo using this imaging technique.

Major Concerns:

None

Minor Concerns:

There are a couple of suggestions for clarification for readers who may not be familiar with specifics in apparatus and/or tissues used in this manuscript.

Page 2, line 95, what is the reason of sublethal irradiation followed by bone marrow transfer? Since the host mice are already double labeled by Mx1/Tomato and aSMA-GFP for imaging purpose, it is difficult to understand the necessity of this procedure without explanations.

Although P-SSCs can be selectively labeled by Mx1/Tomato and aSMA-GFP combination (yellow), Mx1 also labels most of hematopoietic immune cells (red). The Mx1-labeled immune cells may respond to bone injury and may limit clear imaging of P-SSC migration. Therefore, to eliminate endogenously Mx1-labeled hematopoietic cells and to image real-time PSSC migration, irradiation and WT-BMT of Mx1/tom/aSMA-GFP mice prior to imaging is necessary. We clarified this point by adding a note and reference on page 2 Lines 99-102.

Page 2, line 132, is shaving necessary/recommended to tape tubing to mouse abdomen?

We recommend shaving the mouse abdomen for two reasons: 1) This allows you to clean the sight were the needle will be placed for an extended period of time, and 2) the needle is more secure and will not

move while placing the mouse in the restraint.

Page 4, line 207, what is the reason/advantage to use second harmonic generation imaging here?

The benefit of second harmonic generation imaging in this method is to provided a structural reference of the calvaria in combination with fluorescently labeled single cell imaging that cannot be achieved with other imaging methods (i.e. confocal microscopy or uCT).

Page 4, line 218, in which solvent is methylcellulose prepared? PBS?

We use sterile 2% methylcellulose in water (w/v) to cover the entire calvaria. We have added this information to the protocol on page 4, Step 5b-ii (line 232).

Page 5, line 258-263, please refer fig 2A and 2B.

Reference to figures 2A & B have been added to the text. Page 6 line 275.

Page 5-6, between injury and imaging, how the mice have been kept for 24 hours? Was the skin incision closed by nylon sutures and then reopened for imaging?

To clarify this point, we have revised the note in step 4.b.v. on page 4 lines 193-198.

Page 6, line 266, are the white dotted squares in Fig D the same as shown in 0:00 and 1:00 panels in Fig. 2E? If so, 0:00 time point in those two panels do not look the same.

We appreciated the reviewers comment and have replace the 1:00 after CCL5 administration image in figure 2D with the appropriate corresponding image in 2E.

Page 6, Fig 2B/D, are the orientation of Fig 2B and D same? Based on the image shown in 2A and annotation of SS (sagittal suture), one would interpret that injury in Fig 2B was introduced in the right parietal bone, which is different from what shown in other cartoons. The legend for Fig 2C and 2E (but not 2D) says the injury site is located at the top right. It would be less confusing if an image with the same orientation was shown in Fig. 2B.

We have rotated figures 2D and 2E so that the orientation is the same as figure 2B and added additional annotations to clarify figure orientation. The updated figure 2 legend is on page 7 lines 286-302.

We again thank the reviewers for their thoughtful and extremely helpful input and hope that our responses are satisfactory.

Your consideration is much appreciated.

Sincerely,

Laura Ortinau and Dongsu Park